





The role of climate and islands in species diversification and reproductive-mode evolution of Old World tree frogs

Gajaba Ellepola ^{1,2}, Marcio R. Pie ^{3,4}, Rohan Pethiyagoda⁵, James Hanken ⁶ & Madhava Meegaskumbura ¹✉

Large diversifications of species are known to occur unevenly across space and evolutionary lineages, but the relative importance of their driving mechanisms, such as climate, ecological opportunity and key evolutionary innovations (KEI), remains poorly understood. Here, we explore the remarkable diversification of rhacophorid frogs, which represent six percent of global amphibian diversity, utilize four distinct reproductive modes, and span a climatically variable area across mainland Asia, associated continental islands, and Africa. Using a complete species-level phylogeny, we find near-constant diversification rates but a highly uneven distribution of species richness. Montane regions on islands and some mainland regions have higher phylogenetic diversity and unique assemblages of taxa; we identify these as cool-wet refugia. Starting from a centre of origin, rhacophorids reached these distant refugia by adapting to new climatic conditions ('niche evolution'-dominant), especially following the origin of KEIs such as terrestrial reproduction (in the Late Eocene) or by dispersal during periods of favourable climate ('niche conservatism'-dominant).

¹College of Forestry, Guangxi Key Lab for Forest Ecology and Conservation, Guangxi University, Nanning 530004, PR China. ²Department of Zoology, Faculty of Science, University of Peradeniya, Peradeniya, Sri Lanka. ³Departamento de Zoologia, Universidade Federal do Paraná, Curitiba, Paraná 81531-980, Brazil. ⁴Biology Department, Edge Hill University, Ormskirk, United Kingdom. ⁵Ichthyology Section, Australian Museum, Sydney, NSW 2010, Australia. ⁶Museum of Comparative Zoology, Harvard University, Cambridge, MA 02138, USA. ✉email: madhava_m@mac.com

Since Darwin, evolutionary biologists have sought to understand the processes that underlie large-scale diversifications, wherein large assemblages of closely related lineages evolve from a common ancestor^{1–4}. Although several factors may mediate diversification, including geography, ecological opportunity, and key evolutionary innovations (KEI)⁵, the role of the ecological niche, particularly its climatic axes, remains poorly understood^{6–9}.

Two main processes are central to understanding the role of climate in the evolution of geographical distributions: niche conservatism (NC), where species tend to maintain their ancestral climate niche over time^{10–13}; and niche evolution (NE), where species adapt to new climatic conditions^{7–9}. To colonize climatically similar areas when NC predominates, species require optimal climatic conditions to move across erstwhile climatic barriers¹⁴, whereas if NE predominates, species adapting to new conditions can overcome such barriers. Hence, knowledge of how climate niches change over evolutionary timescales can enhance our understanding of the current distribution of lineages⁸.

Rhacophorid tree frogs comprise a spectacular diversification that can be used to test climatic correlates of evolution. Encompassing nearly 6% of global anuran (frog and toad) diversity, with 432 species in 22 genera^{15,16}, rhacophorids occupy a large and climatically variable geographic area, mainly in Asia and a single clade in Africa^{15–18}. Across this range, rhacophorids are distributed in distinct biogeographic regions^{17,18}, which include swaths of continental mainland (East/Southeast Asia, peninsular India, and Africa), continental islands (Japan, Taiwan, Hong Kong, Hainan, Sri Lanka, and Andaman Islands), archipelagos (Sundaland, the Philippines), and montane regions (Himalaya). The northeast region of the subtropical-temperate Asian mainland and islands hold the early-emerging genera, which are thought to have evolved 68–53 mya¹⁷.

Rhacophorid diversity is clustered spatially and temporally^{17–20}. Some regions have greater clade or genus-level diversity (i.e., higher-level diversity), while others have high species diversity. Yet others are depauperate in both respects. In general, areas of high species diversity are regarded as sources of diversification (species pumps), which nourish adjacent areas with lineages that evolved in situ²¹. However, regions with high diversification rates (the net result of speciation and extinction over time) are not always those with high phylogenetic diversity²², because species diversification may occur within just one or only a few clades or genera. Although highly diverse regions exhibit distinctive as well as shared climatic characteristics, the role of climate correlates in driving rhacophorid diversification remains poorly known. Understanding how species' climate niches changed over time will reveal how species dispersed widely from their region of origin and how they adapted in response to different climatic conditions.

Understanding the role of climate is made more complicated, however, by rhacophorids being reproductively diverse. They exhibit four distinct modes: aquatic breeding (AQ; gel-covered aquatic eggs and aquatic tadpoles), gel nesting (GN; gel-covered terrestrial eggs and aquatic tadpoles), foam nesting (FN; foam-covered terrestrial eggs and aquatic tadpoles), and direct development (DD; terrestrial eggs and froglets fully developed at hatching)^{18,19,23}. The likely ancestral mode of nearly all currently recognized genera (except the basal, fully aquatic forms) is GN, while DD and FN appear to be KEIs that enabled rapid diversification¹⁹. Foam nesting (FN) enables rhacophorids to lay large numbers of eggs in more open and drier habitats, where resistance to desiccation is essential¹⁹. Indeed, foam-nesters are characterized by large geographic ranges across potentially xeric and open habitats, making them excellent dispersers¹⁹. Alternatively, terrestrial direct development (DD) allows frogs to lay

eggs in a diversity of humid habitats away from bodies of water. These two reproductive modes (FN and DD) together represent a KEI that facilitated the evolution of nearly half of all known rhacophorid species¹⁹, which occupy warmer but humid climatic conditions. Because geographic ranges of some genera exhibiting FN or DD do not overlap, each mode may represent an evolutionary response to variable climatic conditions in the past. However, the climatic correlates of these reproductive modes are poorly understood, and some of them may represent adaptations to spread across climatic barriers (in the context of NE).

Diversification of ectothermic tetrapods, including anurans, is influenced by climate²⁴. Since rhacophorids are distributed across a climatically variable range and given that their diversity is clustered in space and time^{17,18}, we hypothesize that their diversification and dispersal have a strong climatic context (NE vs. NC), which is also mediated by reproductive mode evolution. This hypothesis generates several testable predictions: (1) Rhacophorid diversity is clustered in climatically similar regions. A clade-level analysis should show the extent to which derived clades have shifted from the climate niches of early-emerging clades as well as the role of NE vs. NC for each clade. (2) Regions with relatively high diversification rates, such as islands and archipelagos, have increased ecological opportunities and are characterized by reproductive modes regarded as KEIs (DD and FN). (3) NE is achieved through reproductive mode evolution if correlated with specific climatic events. Analysis of this prediction will identify reproductive modes that enabled dispersal and diversification into optimal climatic oases such as islands and regions that are geographically disjunct from the center of origin.

Results and discussion

Phylogenetic inference. We constructed an updated phylogeny of the Rhacophoridae by including 415 extant species representing all 22 valid genera (Fig. 1). This phylogeny represents the most complete taxon sampling of rhacophorids to date, which enhances its accuracy and support for testing hypotheses of evolutionary relationship²⁵. Our tree is congruent with many recent clade-level analyses (Supplementary Table 1) and offers relatively high support for most major nodes. It also resolves several long-standing taxonomic discordances within the family^{18,26}. *Buergeria*, *Liuixalus*, *Theloderma*, and *Nyctixalus* constitute early diverging lineages, while the remaining genera comprise two major clades: clade A—*Beddomixalus*, *Gracixalus*, *Kurixalus*, *Mercurana*, *Nasutixalus*, *Philautus*, *Pseudophilautus*, and *Raorchestes*; and clade B—*Chirixalus*, *Chiromantis*, *Feihyla*, *Ghatixalus*, *Leptomantis*, *Polypedates*, *Rhacophorus*, *Rohanixalus*, *Taruga*, and *Zhangixalus*. Clade A is distributed largely across East and Southeast Asia, Sundaland, and the Indian subcontinent, whereas clade B is distributed largely across East and Southeast Asia, Sundaland, and Africa (Fig. 1).

Spatiotemporal patterns of diversification. Rhacophorid diversity is clustered spatially and temporally. Islands and some mainland regions have higher diversity and unique assemblages of taxa (Fig. 2a). Species richness (SR) and phylogenetic diversity (PD) are highest in (1) montane and lowland rainforest areas of Borneo; (2) rainforest areas of peninsular Malaysia; (3) rainforest areas in the southern and northern Annamites of Vietnam; (4) northern Indochinese subtropical forests around Yunnan and east Himalaya; (5) northern and southern montane rainforests of the Western Ghats in India; and (6) montane and lowland rainforests of Sri Lanka. These regions each record more than 15 species per 0.5° × 0.5° global grid cell (Fig. 2a). High correlations between SR and PD within these regions highlight their importance as species pumps and refugia for the family as a whole (Supplementary

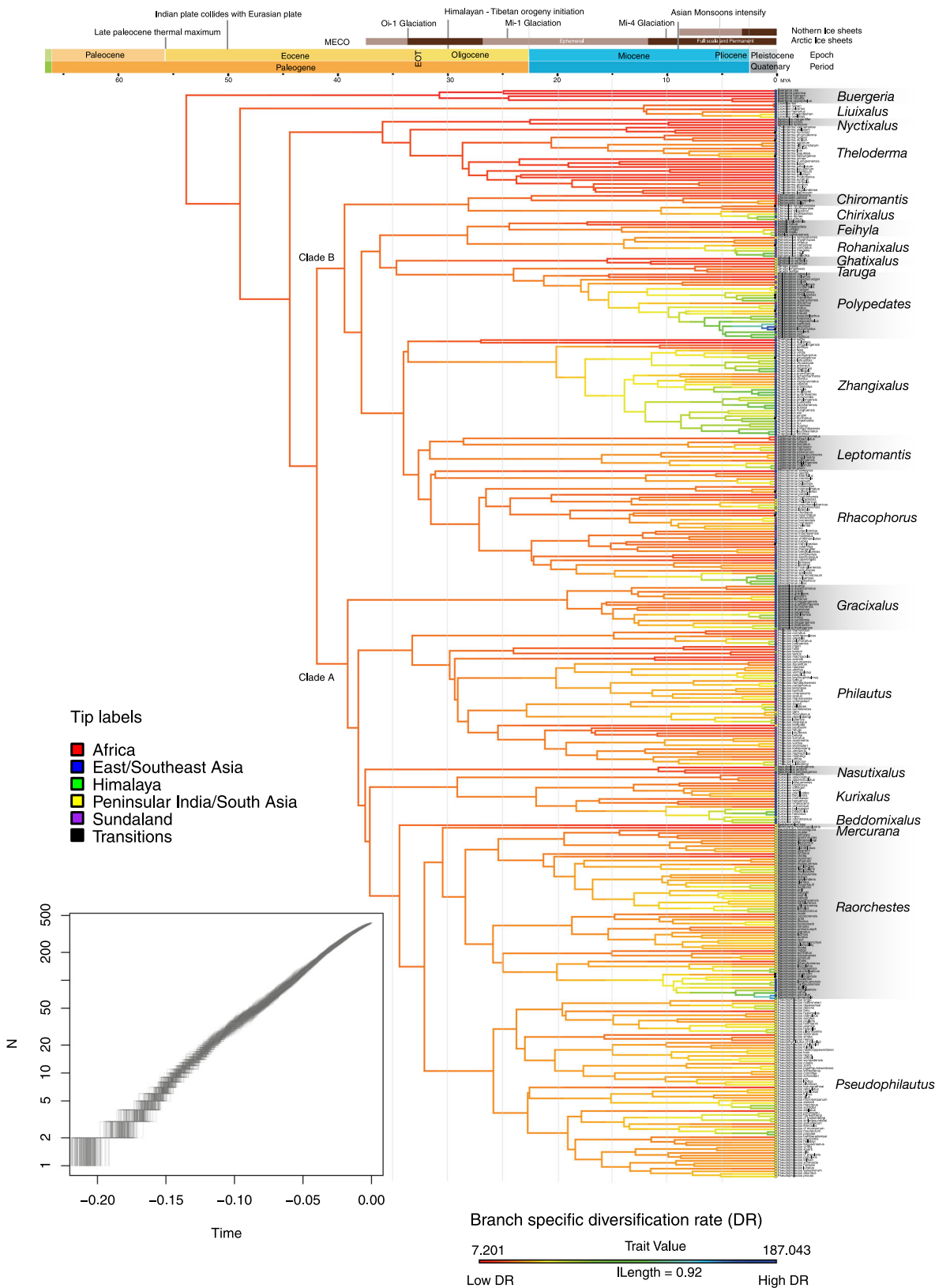


Fig. 1 Complete phylogeny of rhacophorid frogs, with diversification rates (DR) traced across branches. The phylogeny is based on 58 AHE¹⁸ and 315 Sanger sequence data for 415 species. Genetic data were unavailable for 94 species, whose positions in the phylogeny are inferred (constrained) by assessing other taxonomic information. The lineage-through-time plot (LTT; sub-plot) shows a constant rate of diversification, but rates traced on the phylogeny show localized variation, especially among clades (genera): younger taxa have faster diversification rates (cool colors) than older, basal taxa (warmer colors). Colored dots at branch tips indicate the geographic region in which each species occurs; “Transitions” denotes species occurring in two or more regions.

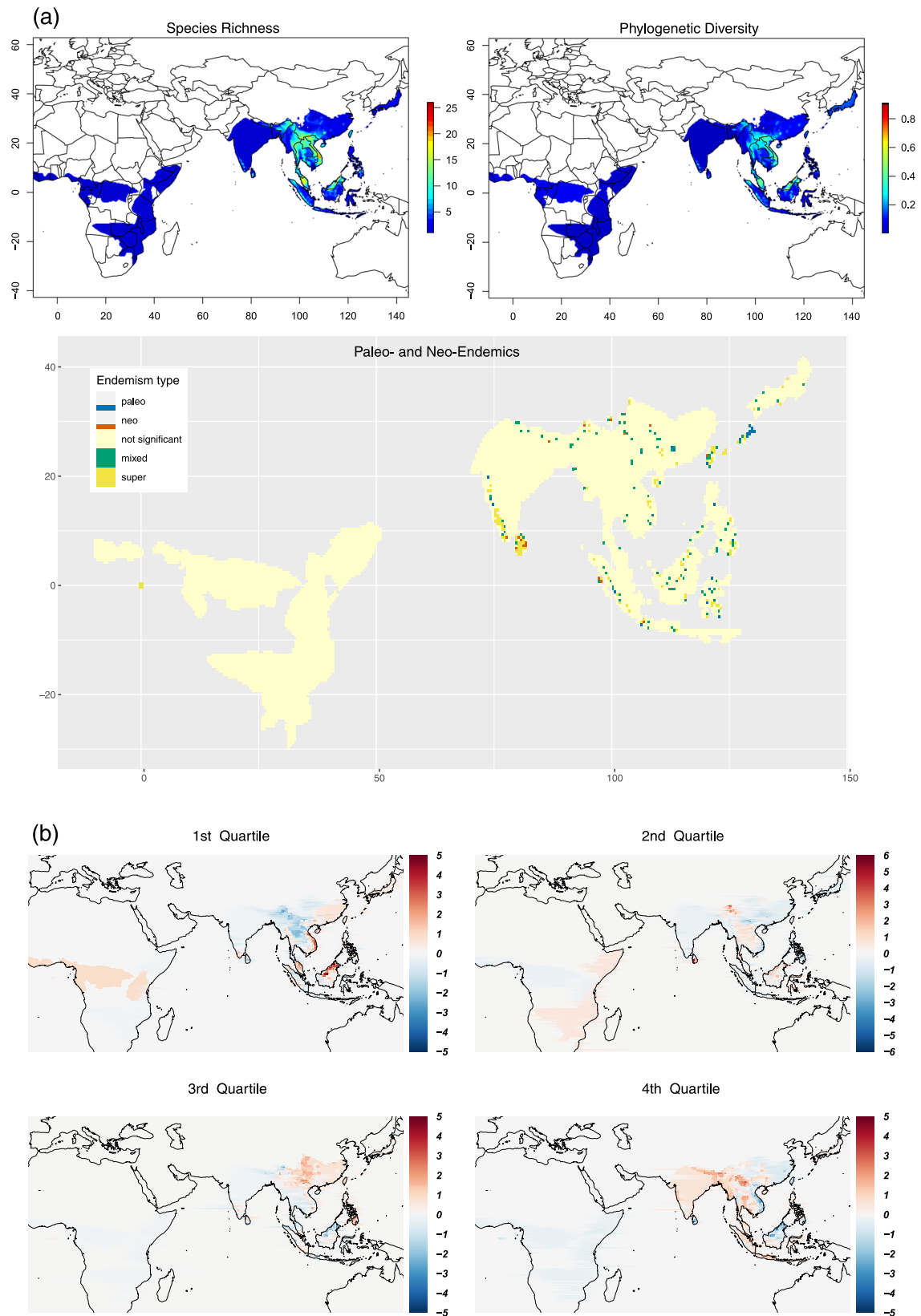


Fig. 2 Patterns of spatiotemporal distribution in Rhacophoridae. **a** Spatial clustering of species richness (SR), phylogenetic diversity (PD), and regions of paleo- and neo-endemism in $0.5^\circ \times 0.5^\circ$ grid cells based on the presence-absence matrices derived from species' geographic ranges (see Methods). SR and PD are highest in the Sunda islands, peninsular Malaysia, Vietnam, the Yunnan-Guizhou plateau area and eastern Himalayas, the Western Ghats of India, and Sri Lanka, which may have acted as refuges and species pumps. **b** Plots of residuals from linear models that evaluate the relationship between $0.5^\circ \times 0.5^\circ$ grid cell richness for each DR quartile, i.e., overall rhacophorid richness. Red colors highlight grid cells with a greater number of species within the respective DR quartile than is predicted under the expectation of a linear relationship with overall richness; blue colors indicate cells with fewer species than predicted. DR values represent the number and timing of diversification events within a lineage: the first DR quartile represents species with low diversification rates (consisting of older lineages having few close relatives), whereas the fourth quartile represents species with faster diversification (having many young and close relatives). Species in the first quartile are maintained in high numbers along the eastern peripheries of the rhacophorid distribution extending towards peninsular Malaysia and Borneo. The distribution of second quartile species supports a hypothesis of early dispersal and diversification events in which dispersal has been towards central Asia, with new species-rich diversifications also forming in East Himalayas and Sri Lanka. In the third quartile, central Asia becomes more diverse. Finally, in the fourth quartile, high-elevation regions along western China and Himalayas become highlighted as sources of recent diversification events. Regions of high SR and PD contain both the oldest and the youngest lineages. These regions may have served as species pumps and refuges during rhacophorid diversification.

Fig. 1). According to the categorical analysis of neo- and paleo-endemism (CANAPE)²⁷, montane islands in east Asia and Sunda islands, the Himalayan mountains of China and India, Vietnam, and the Western Ghats of India are identified in particular as regions of paleo-endemism (Fig. 2a). These regions may have acted as climatic refuges for clades that are present today. The montane islands of Sri Lanka and Indonesia, as well as elevated regions around the Himalayas, depict regions of neo-endemism. We further identify, the montane islands, Western Ghats escarpment, and mountainous areas within Asia as regions of super endemism representative of a mix of most highly significant paleo- and neo-endemic species. Indeed, these regions are widely recognized as global centers of biodiversity^{28–30}, especially amphibian diversity^{31,32}.

Climatic correlates of diversification. The effect of climate on diversification is mediated by other factors, such as the range of ecological opportunities and the particular lineages present at a given location, and thus has a strong geographic context³³. However, geography alone cannot discern the role of climate; similar climatic conditions may occur at different locations at different time periods and affect the evolution of independent lineages. Therefore, to identify the regions of relative climate stability during rhacophorid history, we performed a climate stability analysis as implemented in the R package *climateStability*³⁴. However, we were able to measure relative climate stability only since the Miocene (3.3 Ma), as paleoclimatic data layers extending back to the time of origin of Rhacophoridae are unavailable. Next, to understand patterns of occupation of climate niche space and the climatic conditions under which rhacophorid species evolved, we extracted the mean climatic conditions of 3846 georeferenced coordinates of collecting localities of all species using data for 19 bioclimatic variables from WORLDCLIM 2.0³⁵. We then used the average bioclimatic conditions in a principal components analysis (PCA) based on their correlation matrix, assuming that calculated species means reasonably approximate the realized climate niche of a given species^{9,36}.

The most important dimension of the rhacophorid climate niche (Supplementary Table 2) is dominated by variation in temperature (PC1), particularly during the cold season (BIO6), followed by the mean temperature of the warmest quarter (BIO10) and precipitation seasonality (BIO15). Species from regions with the greatest SR and PD primarily occupy a realized climate niche with cool-wet conditions (Fig. 3). Such conditions, marked by mild temperatures and humid climates, are prevalent in mainland regions (e.g., subtropical China) and mountainous regions in tropical islands characterized by monsoonal climates³⁷. In fact, the temperature regime has remained stable in these regions at least since the Miocene (Supplementary Fig. 2). In

short, rhacophorid diversity is clustered in climatically similar but geographically dissimilar regions (Figs. 2a, 3). As these areas are also characterized by high PD³⁸ and paleo-endemics, they may have acted as refugia during rhacophorid diversification.

Early diversification under NC-dominant cool-wet climatic conditions. Diversification rates (DR) calculated from the DR statistic (see Methods) show localized variation when overlain on the phylogeny, especially in relation to clades: rates are low in phylogenetically isolated lineages that are the result of early speciation events (i.e., early diverging lineages), whereas high rates are associated with members of terminal diverse lineages that originated from more recent speciation events (Fig. 1). We scored and ranked all lineages with respect to their relative phylogenetic isolation as defined by the DR value (higher values represent a greater degree of phylogenetic isolation)³. Then, based on these rankings, we divided DR into quartiles in which the first quartile contains the oldest and least diverse lineages and the fourth quartile contains the youngest and most diverse ones (Supplementary Fig. 3). Subsequent mapping of the residuals of the linear regression between the species richness of each grid cell in each quartile against overall rhacophorid richness at a scale of $0.5^\circ \times 0.5^\circ$ ^{39,40} reveals geographic variation in lineage accumulation through space and time (Fig. 2b). Furthermore, as the metrics SR, PD, DR, and species crown age (SA) are significantly correlated (Supplementary Fig. 1), the spatial analyses yield similar patterns regardless of which metric is used. Species on long branches (i.e., those with the fewest close relatives, especially early diverging lineages; first DR quartile) are prevalent along the eastern periphery of the rhacophorid distribution, extending towards peninsular Malaysia and Borneo. Based on ancestral geographic range reconstructions, Li et al.¹⁷ and Chen et al.¹⁸ conclude that mainland Asia played a significant role in the early diversification of rhacophorids and that ancestors of all early lineages in the Himalaya, peninsular India, Africa, and Sundaland arrived via dispersal from mainland Asia, mostly in the Oligocene. Their conclusion is supported by our finding that the species richness of older lineages is highest in East/Southeast Asia. We further suggest, these being regions of paleo-endemics and given their high PD, that they might also have acted as refuges for Rhacophoridae, especially during the early phases of its evolutionary history.

Reconstruction of variation in speciation rate (DR statistic) onto the maximum clade credibility tree shows that rates have been approximately constant throughout rhacophorid history, with only a few instances of a rate increase or decrease towards the Miocene. This pattern is confirmed by the LTT plot based on 1000 post-burnin trees (Fig. 1). If climatic conditions within East/Southeast Asia were favorable during the period of origin of

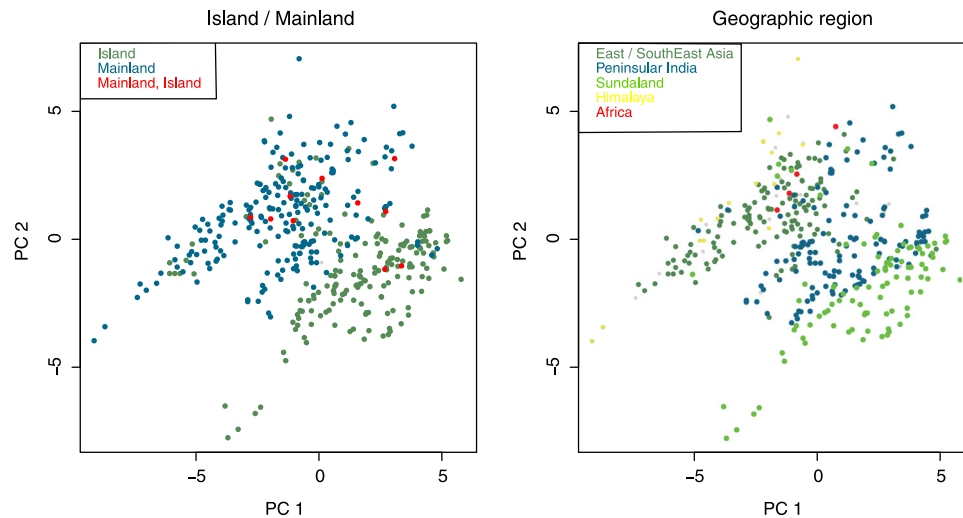


Fig. 3 Climatic space in Rhacophoridae defined by the first two principal component axes of climate niches. Each point represents the average climatic conditions of a single species. Loadings are provided in Supplementary Table 2. PC1 explains 40.5% of the variance and reflects variation in temperature; PC2 explains 23.9% of the variance and reflects variation in temperature and rainfall. Geographically, species in Sundaland are adapted to warm and less-seasonal climates, whereas species from East/Southeast Asia and Himalaya are cool-wet adapted. General patterns indicate that island species are comparatively warm-adapted while mainland species are more or less cool-wet adapted.

the Rhacophoridae, then one might instead expect to see an early burst of diversification^{18,41}. We, therefore, suggest that early climates were less favorable for the diversification of these frogs. This is supported by the fact that the common ancestor of the Asian tree frogs likely arrived from Madagascar around 60–70 mya, possibly via the Indian plate¹⁷ (geological evidence for early India-Asia contact is still lacking), during a relatively warmer, climatically less favorable period⁴². However, assuming that the climatic conditions in which a species occurs reflect the conditions under which it evolved (viz., if NC predominated during early stages), rhacophorids appear to have survived in cool-wet, humid subtropical climates⁴³, mostly towards the eastern periphery of the family's contemporary distribution. Moreover, as most early lineages occur in close proximity to their regions of origin (cool-wet climates), we infer that NC played a major role in early diversification (Fig. 2b; Q1). This claim is corroborated by the fact that the most recent common ancestor (MRCA) and older lineages of Rhacophoridae were aquatic breeders (AQ)^{18,19}, a life history mode that, in rhacophorids, favors humid and cool climatic conditions.

Ecological opportunity would have been a significant factor in enabling the early dispersion and diversification of rhacophorids following their arrival on the Asian plate. Indeed, they dispersed extensively from their region of origin to other parts of Asia, India, Africa, and Himalayas, as well as subtropical and tropical continental islands such as Taiwan, Japan, Sundaland, Philippines, and Sri Lanka^{17,18} during phases of lowered sea level²⁰. Areas with low species richness of old lineages in the first quartile (Fig. 2b) may have experienced extinctions and/or immigration of lineages that had already diversified elsewhere. The overall distribution of species within the second quartile, being similar to regions of the first quartile reaffirms the idea that NC was dominant during early dispersal and diversification. However, species-rich diversifications originating in East Himalayas and Sri Lanka in the second quartile may be attributed to NE as they involve high-elevation areas. Central Asia appears more diverse in the third quartile, but the distribution seems more confined, marking a period of less favorable climate.

Distribution-range expansion is more prominent in the first and fourth quartiles, which suggests that rhacophorids dispersed widely from their region of origin (North/Northeast Asia marked

by cool-wet climates⁴³) to adjacent regions when climatic conditions were favorable for dispersal (Fig. 2b). Such climates have prevailed mainly during the Eocene-Oligocene transition (23–33 mya) and late Miocene (5.3–11.6 mya), when periodic glaciation led to depressed sea levels and the emergence of land bridges^{42,44}, or when lowland dry zones became colder, enabling long-distance dispersal of rhacophorids, followed by subsequent diversification^{41,45}. Dispersals associated with NC might have been further facilitated by increased rainfall associated with the staged, rapid rise of the Himalayas and the consequent strengthening of the Asian monsoonal cycle^{20,46–48}.

NE-dominant diversification. Dispersal of rhacophorids from their center of origin (cool-wet) to the mainland (cooler, seasonal climates) and island refuges (warmer, less-seasonal climates; Fig. 3) requires traversing climatically harsh regions⁴⁹ (especially for dispersal to peninsular India and Africa) and/or sea passages that appear intermittently via land bridges, as in the Sundaland region and between India and Sri Lanka. These intervening areas and land bridges are usually lowland areas with warmer climates. Therefore, apart from dispersing only during favorable periods (NC), crossing such areas periodically would also require adapting to harsh climates (NE). Indeed, the groups most successful at dispersal and habitat utilization did so in association with the evolution of their climatic niche. Climatic correlates of evolution using ES-sim are not statistically significant (Supplementary Table 3), but other analyses suggest that climate played a major role in species diversification. For example, higher disparities shown along PC3 (dominated by high summer temperatures) during the first quartile of diversification in East/Southeast Asia provide initial evidence that after the MRCA colonized this region, its descendants adapted (NE) to increasing summer temperatures (Fig. 4). The corresponding time periods coincide with the Middle Eocene Climatic Optimum (MECO), a global warming event that occurred about 40 mya⁵⁰. The subsequent Eocene-Oligocene transition, underscored by Oi-1 glaciation, resulted in a global cooling event⁴² that brought about sea level lowstands^{42,44} and facilitated the dispersal of these warm-adapted MRCAs to adjacent refuges via intervening climatically harsh areas. Adaptation to warmer climatic conditions during the

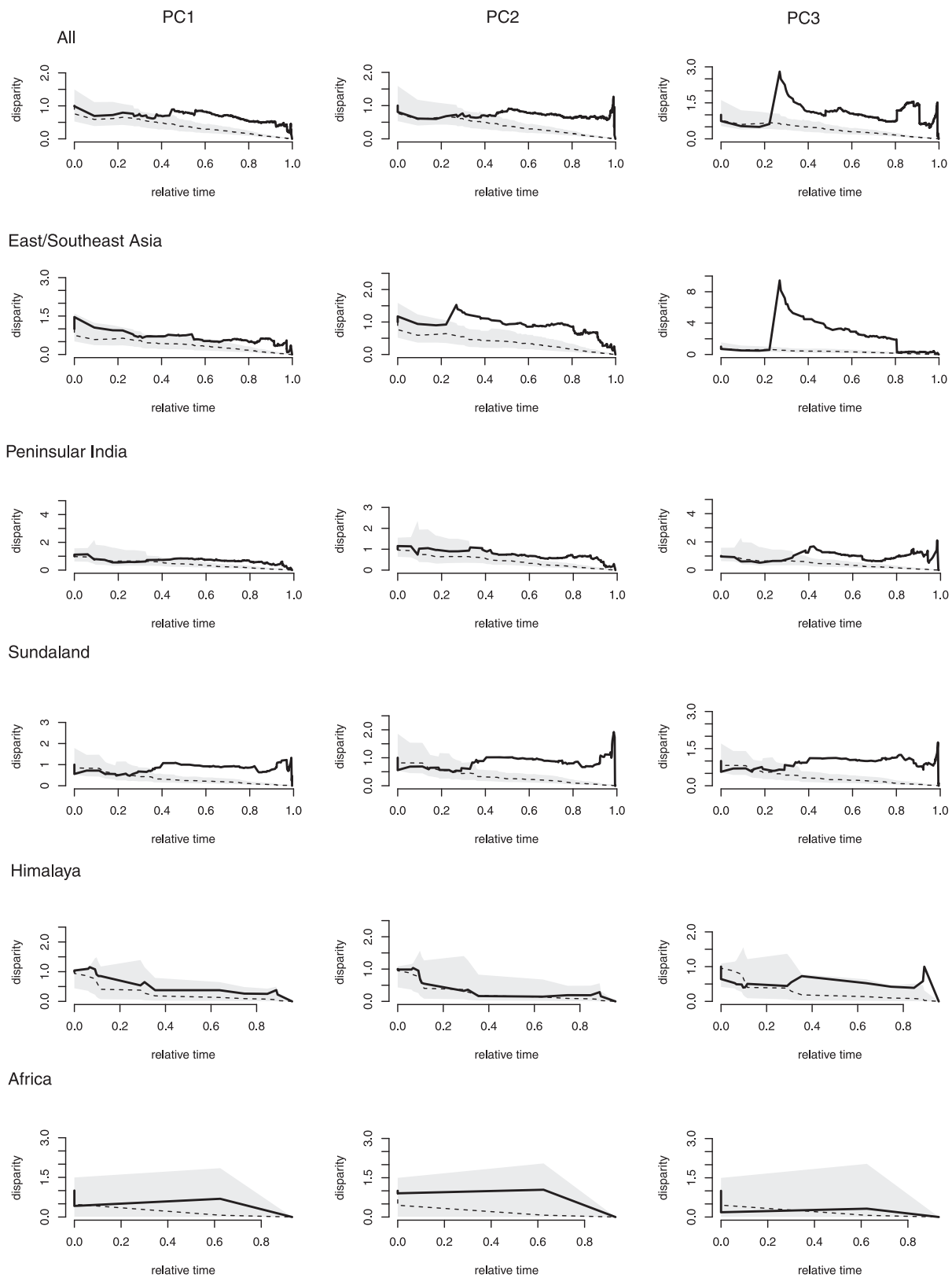


Fig. 4 Relative disparity-through-time (DTT) plots of PC scores representing rhacophorid climate niches. Solid lines indicate observed DTT values; dashed lines and the corresponding polygons represent averages and 95% confidence intervals, respectively, of the expectations given a constant accumulation of disparity over time based on 999 pseudoreplicates. The disparity of climate niche evolution is higher in all biogeographic regions except Africa, especially during the second half of the diversification. Markedly higher levels of disparity are observed in PC3 (higher summer temperature) early in the evolution of species from East/Southeast Asia and peninsular India, and recently in species from Sundaland.

MECO thus might have been a major evolutionary advancement in common ancestors showing high dispersal capabilities during the early stages of their diversification. Elevated rates of climatic niche evolution in species having broad distributional ranges further support this finding (Supplementary Table 4).

Variation in rates of climate niche evolution among biogeographic regions indicates the great extent to which this trait depends on the relative location of the species involved (Supplementary Table 4). For example, after the Eocene-Oligocene transition, climatic conditions in East/Southeast Asia became colder with the Tibetan-Himalayan orogeny (ca. 30 mya), which, in turn, initiated monsoon cycles^{46,47}. Species that continued to occupy cool-wet climates in East/Southeast Asia further adapted towards cooler climate niches, punctuated by seasonal variation (Fig. 5). In contrast, species that dispersed towards lower latitudes, in particular, Sundaland and peninsular India, invariably had to adapt to climate niches associated with higher temperatures to survive in warmer tropical environments.

The alternative, bin-based ancestral reconstruction analysis of niche evolution based on the R package *nichevol*⁵¹ reveals niche expansion in many rhacophorid genera (Supplementary Fig. 4). This result is congruent with those of NE-based traitgrams. Certain genera showing niche expansion also seem to show niche retraction, possibly due to niche specialization seen in a few species within those genera. This analysis supports the idea that suitable climates for ancestors prevailed around the subtropical region and mountainous areas (Fig. 5) and that species seem to have evolved their niches while dispersing into new habitats (i.e., towards tropics, further towards temperate areas or, while moving towards low-lying areas from their regions of origin).

Role of islands on diversification. Island formation during the Miocene⁵² also played a significant role in shaping rhacophorid diversification. In general, a continental climate has characteristics associated with areas within a continental interior, unlike island climates, which typically are influenced by surrounding bodies of water. These differences may affect species composition⁵³. Accumulation of numerous young rhacophorid lineages in island regions during the Miocene suggests the potential role of islands as species pumps for relatively young species (high SR) as well as refuges (high PD)^{21,54} (Fig. 2b; Q4). In the PCA plot of climate niche space, island species tend to be associated with intermediate (in subtropical islands) to warmer temperatures (in tropical islands), while mainland species tend to be associated with colder climates influenced by seasonality (Fig. 3). Islands tend to have stable, i.e., less seasonal, climates relative to mainland environments⁵⁵, which may buffer island species against the effects of a changing climate.

Climate stability on islands, however, need not imply optimality. Species dispersing to islands may need to adapt to novel climatic niches. The higher rates of climate niche evolution for species living on both islands and the mainland, compared to the only-island and only-mainland species, suggest that climate niches evolved extensively in species that show long-distance dispersal (Supplementary Table 5). Interestingly, island species are derived from recent speciation events and have a mainland origin (Supplementary Fig. 5). Island species have higher rates of evolution along PC1 and PC2, whereas mainland species tend to have higher rates along PC3 (Supplementary Table 5). In the context of Rhacophoridae as a whole, the pioneering ancestors of island clades may have been warm-adapted, low-elevation forms that subsequently colonized relatively warm areas (i.e., islands), whereas mainland species that remained in ancestral niches underwent further diversification in situ. However, species that

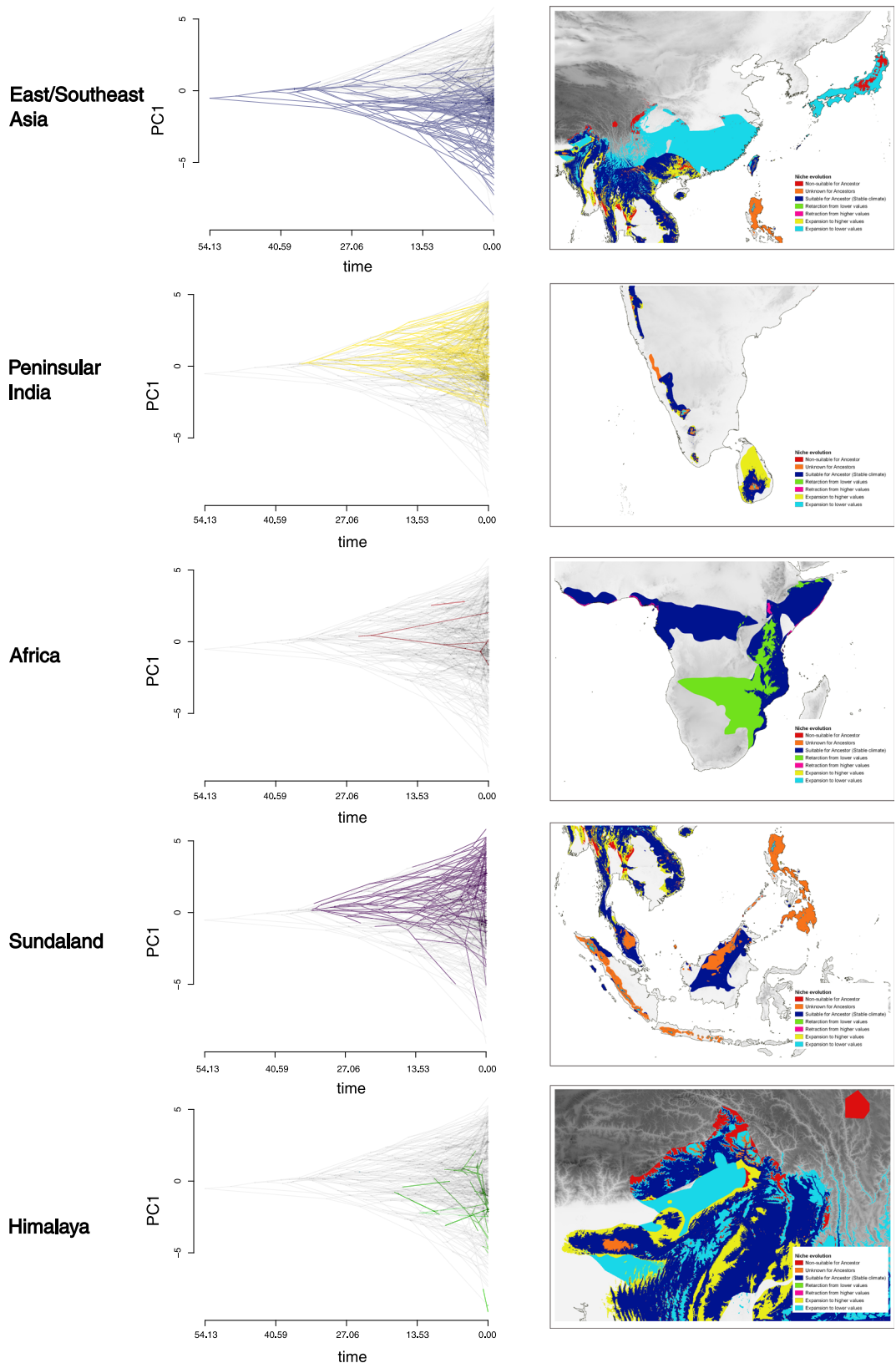
successfully colonized islands show higher rates of climate niche evolution than mainland species (Supplementary Table 5), which suggests that novel ecological opportunities provided by mountains and other complex topographic features within islands may facilitate their high diversity^{5,41,56}. According to niche conservatism, because islands are geographically and environmentally heterogeneous, species may be able to maintain their optimal environment and enhance their chance of persistence simply by dispersing across relatively small distances, especially on topographically complex islands⁵⁷. This may explain how rhacophorids have diversified under less conducive, relatively warmer, and less seasonal climatic conditions on islands by either NE, NC, or both. Some of these species, however, might at some point recolonize and re-establish in their continental ancestral area if suitable environmental and ecological conditions return^{41,58} (Supplementary Fig. 5).

Climate and the evolution of reproductive modes. A comparison of diversification rates associated with different reproductive modes and among regions (Fig. 6a) reveals that fully aquatic breeders (AQ) are found only in cool-wet East/Southeast Asia¹⁹, whereas lineages that dispersed from there to other regions tend to have more terrestrial reproductive modes (direct development, DD; and foam nesting, FN). Moreover, these terrestrial modes are associated with higher diversification rates in all regions. We suggest that a shift from a fully aquatic reproductive mode to more terrestrial modes, but especially to DD and FN, facilitated the dispersal of rhacophorids from their center of origin into optimal but distant climatic oases such as islands. This scenario is corroborated by the pattern of climate niche occupation of the four reproductive modes: fully aquatic (AQ) and semi-aquatic (GN) species are confined to relatively cool-wet East/Southeast Asia and adjacent subtropical and temperate islands, whereas the more terrestrial modes are confined to warmer climates mostly found in tropical islands (mainly Borneo, Java, Sumatra, Philippines, and Sri Lanka), which lie within the intertropical convergence zone (Fig. 6b).

After they colonized East/Southeast Asia, early-emerging aquatic-breeding rhacophorids evolved new breeding strategies—gel nesting (GN), foam nesting (FN), and direct development (DD)—which are KEIs in the clade^{18,19}. Species bearing more terrestrial reproductive modes tend to have broader climatic niches, and hence, wider climatic tolerance ranges, which is suggestive of greater dispersal capabilities. For example, rates of climate niche evolution are higher in FN and DD, whereas the climatic niche in AQ has been more conservative (Supplementary Table 6).

Traitgrams of different reproductive modes suggest that GN may have evolved in association with the MECO global warming event during the early Eocene, more than 40 mya⁵⁰ (Fig. 6c). Gel nesting (GN), which is characterized by gel-covered, terrestrial eggs, and free-living aquatic tadpoles²³, can be regarded as an initial transitional stage in the evolution of a fully terrestrial life history¹⁹. Adoption of this reproductive mode has enabled NC-dominant dispersal of rhacophorids into relatively cool-wet areas within close proximity to ancestral climatic niches of AQ (Supplementary Fig. 6). In addition, results of bin-based ancestral reconstructions confirm that GN genera also show some evidence of niche expansion (Supplementary Fig. 4).

Traitgrams of the more terrestrial modes FN and DD suggest that they evolved after GN but during the same geological period. Thus, increasing temperatures during MECO may have promoted the adoption of novel modes of reproduction, which equipped rhacophorids for more terrestrial life. The subsequent Eocene-Oligocene transition, marked by depressed sea levels, land bridge



emergence^{42,44} and cooler lowland dry zones, then enabled long-distance dispersal of terrestrial-breeding (FN and DD) lineages. The bin-based ancestral state reconstruction analysis reinforces this scenario: niches of most FN and DD forms evolved to tolerate warmer conditions, although several species show evidence of

niche retraction as well. Overall, these results indicate that FN and DD forms were successful dispersers, insofar as they were able to overcome the ancestral dependence on aquatic habitats while evolving climate niches (NE) adapted to broader climatic conditions.

Fig. 5 Climate niche evolution in different geographic regions. The first column depicts variation among biogeographic regions in the rate of evolution of the climatic niche explained by the first principal component axis (PC1) of average climatic conditions for each rhacophorid species. The X-axis corresponds to the approximate age of origin of rhacophorid clades to the present (segmented into quartiles); nodes indicate the inferred climatic niches for the most recent common ancestor of the extant taxa defined by that node. Positive values along the Y-axis represent warmer climates; negative values represent colder climates. Gray branches in the background of each plot indicate the overall climatic niche evolution of rhacophorids along PC1. Divergent branches are more frequent near the present time. While species in East/Southeast Asia (blue) and Himalaya (green) have evolved towards colder climatic conditions and those in Sundaland (purple) and peninsular India (yellow) have evolved towards warmer conditions, species in Africa (red) have not deviated much from their ancestral climate niche. The second column represents niche expansion or retraction compared to its ancestor within the accessible area of Rhacophoridae. BIO6 and BIO10, the two most dominant variables of the rhacophorid climatic niche, are represented. Suitable climates for ancestors prevailed around the subtropical region and mountainous areas; climate niche evolution is evident as species disperse towards the tropics or further into temperate areas or move towards low-lying areas.

Conclusions

The spatial distribution of rhacophorid species is patchy: islands and some mainland regions have higher diversity and unique assemblages of taxa, which contain both older and young lineages. This patchiness can be explained in the context of climate, ecological opportunity, and KEIs. Regions of cool-wet climate may have acted as climatic refuges (high PD regions and regions of paleo-endemics). They are separated from one another by warmer, climatically harsh, low-lying regions and/or sea passages. Lineages overcame these barriers in two main ways: by adapting to harsh climates (NE) or dispersing only during favorable periods (NC). Key evolutionary innovations, such as shifting from a fully aquatic reproductive mode to more terrestrial modes, further facilitated the diversification and dispersal of rhacophorids through these climatically less favorable areas. Finally, ecological opportunity in the form of empty niches seems to have elevated diversification rates on islands, offsetting constraints caused by their less favorable (warmer) climatic conditions. For rhacophorid frogs, climate refuges, ecological opportunity, KEIs, long periods of time to adapt to climatic conditions, and climate niche evolution have combined to promote and sustain a remarkable diversification.

Methods

Comprising 6% of global amphibian diversity, rhacophorid tree frogs occupy a climatically variable geographic area ranging from tropical and subtropical Asia, its continental islands and archipelagos, to Africa. We carried out a series of analyses based on a complete species phylogeny for Rhacophoridae using a combination of phylogenetic inference and phylogenetic imputation to determine how climate has shaped the diversification and dispersal of this charismatic group.

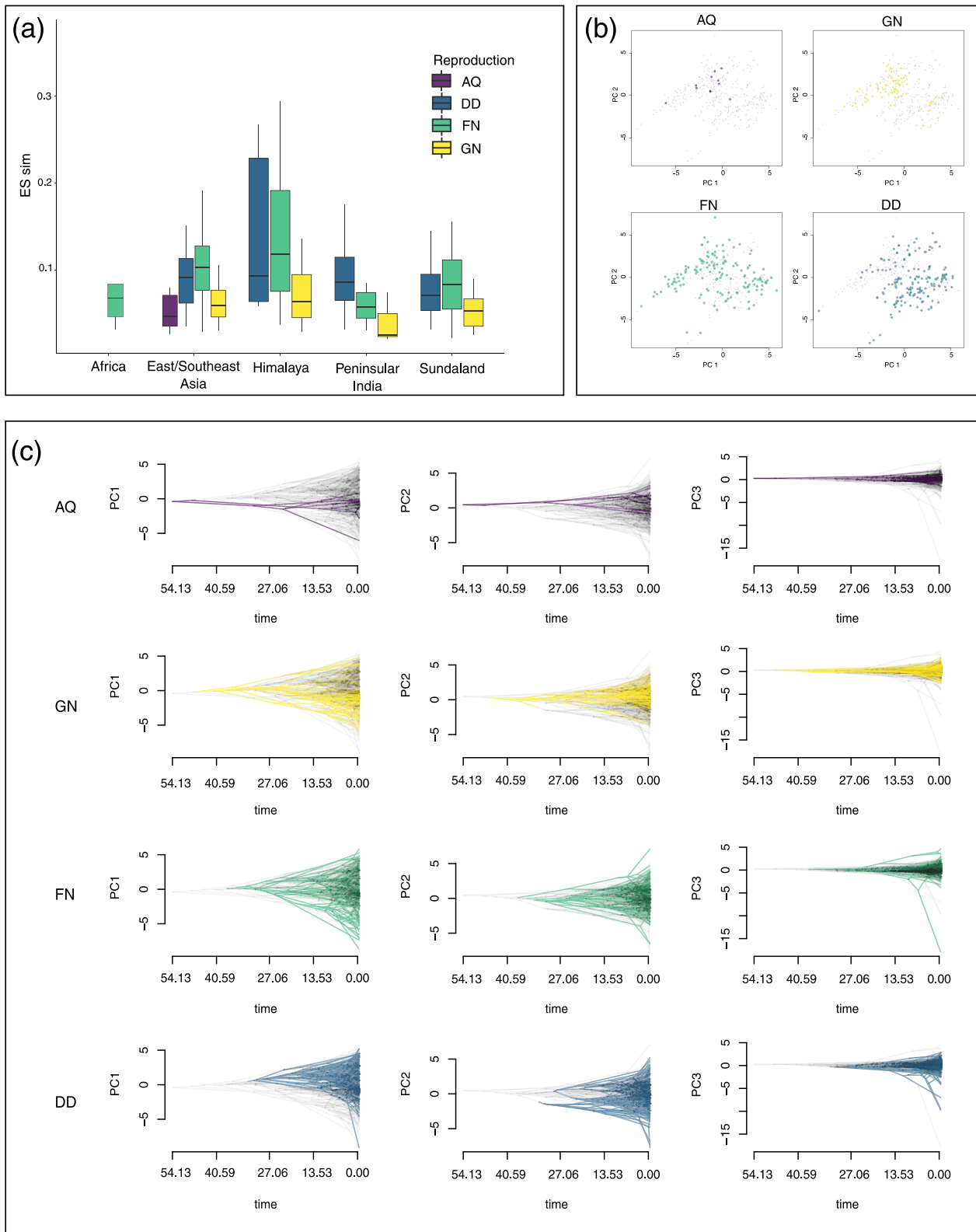
Phylogenetic inference. Extensive taxon sampling is important in phylogenetic systematics; it increases the accuracy and support of evolutionary relationships²⁵. Hence, we derived an updated phylogeny of the family Rhacophoridae with the most complete taxon sampling used to date: 415 extant species representing all 22 genera. Although previous studies have resolved many of the earlier controversies in rhacophorid phylogeny (Supplementary Table 1), taxonomic discordances persist¹⁸, hindering the testing of hypotheses for major evolutionary questions. Moreover, the genetic data available for different rhacophorid lineages are uneven, ranging from none for some species to whole-genome sequences for others, which leads to incomplete taxon sampling. We took three main steps to derive a complete species-level phylogeny: (i) establish a phylogenomic backbone, (ii) compile Sanger sequence data of non-chimeric sequences, and (iii) add species without genetic data using phylogenetic imputation⁵⁹. We began by reanalysing the anchored hybrid enrichment dataset (AHE) of Chen et al.¹⁸. Although there was strong support for most branches of the rhacophorid tree, one clade (comprised of *Pseudophilautus*, *Kurixalus*, and *Raorchestes*) proved recalcitrant; it was unstable in species-tree analyses. We estimated Maximum Likelihood trees for each locus using RAXML 8.2.12⁶⁰; branch support for each gene tree was based on 50 bootstrap replicates. Preliminary analyses indicated that the source of instability was the position of *Nasutixalus*, given that a species tree without that terminal using ASTRAL III v.5.7.3⁶¹ yielded 100% local posterior probabilities for the relationship among *Pseudophilautus*, *Kurixalus*, and *Raorchestes*. We, therefore, enumerated the loci that supported each of the three alternative topologies, as well as the corresponding average bootstrap values of the loci supporting each of them. Given that one of the alternative topologies tended to be more strongly supported by loci with higher average bootstraps (Supplementary Fig. 7), that topology was chosen for downstream analyses.

Once a stable backbone tree was obtained, we compiled all Sanger sequence data available from GenBank (last accessed January 2021), which included 315 rhacophorid species (number of species/genus in parentheses): *Beddomixalus* (1), *Buergeria* (3), *Chirixalus* (2), *Chiromantis* (3), *Feihyla* (4), *Ghatixalus* (3), *Gracixalus* (9), *Kurixalus* (17), *Leptomantis* (10), *Liuxalus* (6), *Mercurana* (1), *Nasutixalus* (3), *Nyctixalus* (3), *Philautus* (31), *Polypedates* (14), *Pseudophilautus* (56), *Raorchestes* (59), *Rhacophorus* (32), *Rohanixalus* (2), *Taruga* (3), *Theloderma* (25), and *Zhangixalus* (28; see Supplementary Table 7). Sequences were obtained for seven gene fragments: mitochondrial loci 16S, 12S, and *cyt-b*; and nuclear loci *BDNF*, *Rag-1*, *rhod*, and *Tyr*. Each locus was aligned separately using MUSCLE⁶² as implemented in MEGA v.6⁶³. Sequences of all fragments were then concatenated, with a total alignment length of 3923 base pairs (bp).

We obtained complete species-level trees by using the two-stage Bayesian approach PASTIS⁵⁹. This method uses as inputs a backbone topology based on molecular data, a set of taxonomic postulates (e.g., constraining species to belong to specific genera or families), and user-defined priors on branch lengths and topologies. Based on these inputs, PASTIS produces input files for MrBayes 3.2.5⁶⁴, which generates a posterior distribution of complete ultrametric trees that capture uncertainty under a homogeneous birth-death prior model of diversification and placement constraints. We used PASTIS version 0.1-2, with functions from the APE 5.4⁶⁵ and CAPER 0.2⁶⁶ packages. There are two main assumptions to this approach: (i) taxonomic groups (e.g., genera) are monophyletic unless there is evidence (i.e., genetic data) that suggests otherwise; and (ii) reasonable edge-length and topology priors (i.e., birth-death models) exist. PASTIS has been used to provide large-scale trees of several higher-level taxa, including birds⁶⁷, squamates⁶⁸, sigmodontine rodents⁶⁹, and amphibians⁷⁰. Thomas et al.⁵⁹ categorize species into three types: type 1 species have genetic information (i.e., genomic data + Sanger sequencing data); type 2 species lack genetic information but are congeners of a species with genetic information; and type 3 species lack genetic data and are members of a genus that lacks genetic data. In our dataset, we have 321 (genetic data present) and 94 (genetic data absent; Supplementary Fig. 8) species exclusively from types 1 and 2, respectively. Our backbone tree was established using the anchored hybrid enrichment dataset¹⁸. Species without genetic data are constrained to their closest relatives based on morphology as indicated in published literature (Supplementary Table 8) and the best partitioning scheme for the Sanger dataset was determined using PartitionFinder2⁷¹. The general time-reversible model with an invariable gamma rate for each partition, birth-death as a prior probability distribution on branch lengths, fixed extinction-rate priors, and exponential net speciation rate priors were assigned to the alignment and constraints and was run on MrBayes 3.2.5 for 20 million generations to obtain the posterior distribution of final ultrametric trees. Convergence was assessed by inspecting the log-output file in TRACER v.1.6⁷² and by ensuring ESS values were greater than 200. The first 10% of the trees were discarded, and the post-burn-in trees were used to infer the maximum clade credibility tree using TREEANNOTATOR v.1.10.4⁷³. The maximum clade credibility tree, as well as a set of 1000 post-burn-in topologies (Supplementary Data 1), were retained for further analyses (see below).

To examine the temporal context of divergence and correlate it with geological and climatic events, we estimated divergence times among lineages in a separate run of the above-partitioned dataset in MrBayes 3.2.5⁶⁴. We initially used the lognormal relaxed clock model with default clock rate priors and, subsequently, the default strict clock model. The lognormal relaxed clock model showed the greatest fit and was used for further analysis. We calibrated the tree using two literature-based, molecular-estimated points from Meegaskumbura et al.³⁹ and Chen et al.¹⁸ (viz., the age of the MRCA of extant *Pseudophilautus*, 21.93–45.14 mya; and the age of the MRCA of clade A, 31.65–40.53 mya, respectively).

Testing for variation in rates of lineage diversification. We tested for potential correlates of speciation rates using ES-sim, a semi-parametric test for trait-dependent diversification analyses⁷⁴. Instead of modeling the relationship between traits and diversification, ES-sim tests for correlations between summary statistics of phylogenetic branching patterns and trait variation at the tips of a phylogenetic tree. It uses the DR statistic⁶⁸, a non-model-based estimator of speciation rate that



is computed for a given species, as a weighted average of the inverse branch lengths connecting the focal species to the root of the phylogeny (e.g., the root-to-tip set of branches). The use of tip-specific metrics of speciation rate may provide an alternative to parametric state-dependent diversification due to the elevated rates of false-positive results, given that heterogeneity in diversification rates of the underlying phylogeny could bias inferences of associations between traits and diversification regardless of their underlying relationship⁷⁵. Simulations show that the use of ES-sim for continuous traits shows equal or superior power to QuaSSE⁷⁴. In addition, given that they are computationally

efficient, tip-specific metrics make it feasible to explore the impact of phylogenetic uncertainty. ES-sim was implemented using the code provided by Harvey & Rabosky⁷⁴ (available at <https://github.com/mgharvey/ES-sim>) and we initially assessed variation in speciation rates among lineages by mapping variation in the DR statistic along the maximum clade credibility tree using the “contmap” function in PHYTOOLS 0.7-47⁷⁶. Given that the DR statistic tends to focus more on processes closer to the present, we compare those results with lineages-through-time (LTT) plots using 1000 alternative trees using the “mltt.plot” function in APE.

Fig. 6 Climatic correlates of different rhacophorid reproductive modes. **a** Box plot showing diversification rates (DR) associated with alternate reproductive modes in different biogeographic regions (aquatic breeding, AQ; gel nesting, GN; foam nesting, FN; and direct development, DD). Species having FN and DD show high diversification rates. **b** PCA plots depicting climate niche occupation of species that utilize the above four reproductive modes. Aquatic breeders display a conservative (narrow) occupation of climatic niche space, whereas FN have the broadest niche. DD are restricted mostly to warmer but humid and less seasonal climates. **c** Variation in the rate of evolution of the rhacophorid climate niche explained by the first three principal component axes (PC1-PC3) of average climatic conditions for each reproductive mode. Early AQ shows a pattern of niche conservatism whereas GN, FN, and DD, which have facilitated the evolutionary transition of rhacophorids to more terrestrial life, appear to have evolved their climate niches during relatively warmer early Eocene (40 mya) conditions. Newly evolved reproductive modes show a pattern of broadening their climate niches subsequent to the Eocene-Oligocene transition (23–33 mya), which was marked by favorable climatic conditions.

Spatiotemporal patterns of rhacophorid diversification. We downloaded distribution ranges as spatial-data polygons from IUCN (2020)³⁹ <http://www.iucnredlist.org/technical-documents/spatial-data> for all available rhacophorid species and transformed them into a presence-absence matrix (PAM) by using a $0.5^\circ \times 0.5^\circ$ global grid using the function “lets.presab” in R package letsR v.3.2⁴⁰. Species richness (SR) was visualized as species richness values per cell on a world map by applying the function “plot” in letsR. Using the maximum clade credibility tree, we calculated phylogenetic diversity (PD), determined as the sum of all co-occurring species branch lengths⁷⁷ within each cell, by applying the function “lets.maplizer,” and obtained a raster to map geographic patterns of PD. Similarly, geographic distribution maps were created for both the DR estimated above⁷⁴ and species crown age (SA), estimated as the length of the terminal branch subtending each species until the most recent speciation event, to visualize spatial patterns of diversification.

To identify regions that may have served as refuges and species pumps in Rhacophoridae, we performed a categorical analysis of neo- and paleo-endemism (CANAPE)²⁷. CANAPE integrates a phylogenetic tree with a community (species \times sites) matrix to infer if endemic areas are so because of recent speciation (neo-endemism), because they harbor old lineages that have mostly gone extinct in other areas (paleo-endemism), or if they are a mixture of both. The analysis was performed following the steps indicated in the R package canaper v.0.0.1²⁷. We used species richness in the PAM object derived from the above $0.5^\circ \times 0.5^\circ$ grid cell as the community matrix and the maximum clade credibility tree obtained from above as the input phylogenetic tree.

As many young (recent) lineages and close relatives attain high values of DR, and those with few close relatives (older/basal lineages) yield lower values (Fig. 1), DR allows us to effectively score all lineages with respect to their relative phylogenetic isolation³. As the above metrics (SR, PD, DR, and SA), especially DR and SA, are significantly correlated (Supplementary Fig. 1), the spatial analyses produce more or less similar patterns regardless of the metric assessed. In the main text, we, therefore, focus on results using DR values. Following Kennedy et al.³, we used the species ranks of DR to divide our distributional database into quartiles. The first quartile contains the oldest and least diverse lineages, while the fourth quartile contains the youngest and most diverse ones (Fig. 2b). We subsequently generated maps of species richness at the $0.5^\circ \times 0.5^\circ$ scale for each quartile using the “lets.maplizer” function in the package letsR. Running a linear regression analysis between grid cell richness of each quartile against that of the overall rhacophorid richness in the cell enabled us to visualize areas that have accumulated a higher- or lower-than-predicted number of species in each DR quartile. Alternatively, this reveals geographic variation in lineage accumulation through space and time. Moreover, a relative and distinct increases in diversifications within the same regions between quartiles would support the idea of NC-dominant early dispersal and diversification. Finally, to explicitly test whether islands serve as species pumps, we used island/mainland as a binary trait and ran ES-sim on 100 potential topologies. Due to the highly correlated nature of DR and SA (Supplementary Fig. 9), it can be assumed that each quartile also represents the temporal aspect of diversification.

To further investigate species accumulation through time in different biogeographic regions (East/Southeast Asia, Sundaland, peninsular India, Himalaya, and Africa), we used subsets of the rhacophorid phylogeny based on geographic region and assigned birth-death models of diversification under four conditions for the birth and death rates specified in the package RPANDA⁷⁸. Best models were selected for each biogeographic region based on AICc values, and diversity through time was visualized using the function “plotdt” in RPANDA (Supplementary Fig. 3).

We also performed an analysis of climate stability as implemented in the package climateStability v.0.1.3³⁴ to identify regions of stable climate during the evolutionary history of Rhacophoridae. We used the climatic layers that are currently available at <http://www.paleoclim.org/>, which only spans up to the Pliocene (3.3 Ma), and performed niche stability analysis for the uneven time scale as implemented in the package. The time period from the Pliocene to the present would represent diversification and dispersal that took place approximately in the fourth quartile. The climate variables BIO1 (mean annual temperature) and BIO12 (annual precipitation) were used to calculate deviation-through-time slices, and we used these deviations to estimate relative climate stability (Supplementary Fig. 2). However, this analysis is limited to the Miocene-present time period due to the unavailability of paleoclimatic layers beyond this period.

Ecological and biogeographic data. Information on the geographical distribution of rhacophorid species derived from occurrence records was obtained from the GBIF database (<https://www.gbif.org>) using RGBIF v.1.4.0⁷⁹ in R v.3.6.1⁸⁰. Distribution data for species not represented in GBIF were obtained directly from the literature and IUCN species range maps. The final distribution dataset comprised 3846 geographical coordinates of all species. Nearly 65% of those species ($N = 273$) were represented by single-occurrence records. This is not uncommon in compilations of this nature^{9,36} and reflects the high degree of local endemism of rhacophorid species. Information on 19 bioclimatic variables for each occurrence point were obtained from WORLDCLIM 2.0³⁵ using the “extract” function in RASTER v.3.0-7⁸¹. Mean values for each bioclimatic variable for each species are provided in Supplementary Data 1. We then used the average bioclimatic conditions in a principal components analysis (PCA) based on their correlation matrix. The axes to be retained for further analyses were determined using the broken-stick method as implemented in VEGAN v.2.5-6⁸². We assume that the measured species means are a reasonable approximation of the realized climatic niche of the species^{9,36}.

Climatic correlates of rhacophorid diversification. When implementing ES-sim⁷⁴, we used 100 simulations to build the null distribution of trait-speciation associations for significance testing. The designated potential correlates of speciation rates were the first three principal components of the climatic niches, mean elevation, and whether these species were island endemics. To account for phylogenetic uncertainty, we repeated each analysis for 100 potential topologies. Analyses were carried out separately for each potential correlate (Supplementary Table 3).

We assessed the extent to which species traits had accumulated over time in each biogeographic region (i.e., climatic niche evolution; NE along each PC axis) by using disparity-through-time (DTT) plots⁸³, with expected disparities calculated based on 1000 resamplings using the “dt” function in GEIGER v.2.0.6.2⁸⁴ and with phenograms (projections of the phylogenetic tree in a space defined by phenotype and time) using the “phenogram” function in PHYTOOLS. Biogeographic categorizations for these analyses are based on Chen et al.¹⁸. Here, East/Southeast Asia includes mainland China and subtropical islands such as Hainan, Taiwan, and Japan; Sundaland includes peninsular Malaysia and islands such as Borneo, Sumatra, Java, and Philippines; and peninsular India includes mainland India and Sri Lanka.

We also used an alternative approach to testing climatic niche evolution in Rhacophoridae by running the niche evolution analysis implemented in the R package nichevol v.0.1.19⁵¹. This allowed us to assess climatic niche evolution against all 19 bioclimatic variables as well as estimate the phylogenetic uncertainty associated with our results of niche evolution. This method relies on the ancestral reconstruction of ecological niches by using a bin-based approach that incorporates uncertainty in estimations. Compared to other existing methods, it reduces the risk of overestimation of amounts and rates of ecological niche evolution⁵¹. However, since the current dataset does not indicate the variance of occurrence records for most of the species ($N = 273$, as many species represent point endemics), we categorized all occurrence points into their specific genera to carry out the analysis. *Beddomixalus*, *Mercurana*, and *Nasutixalus* were removed from the analysis, as the numbers of occurrence records for these genera were insufficient for estimating data variance. The IUCN spatial distribution polygons for each genus and 19 bioclimatic variables were used to carry out the analysis. Initially, we explored the configuration of variable values in the accessible area (M) and occurrences of species as provided by the code. Then, variable values in M were sorted into multiple classes (bins), and, using values in occurrences, the presence or absence of the species in each bin was tested. Values of characters are 0 = absent, 1 = present, and ? = unknown (uncertain). Ancestral reconstructions of ecological niches (represented by 19 bioclimatic variables) were performed using both the MCC tree and 1000 posterior trees so that it accounts for the uncertainty of our results. Reconstructions were performed using maximum parsimony and maximum likelihood methods. Results were similar, although variation was higher in maximum parsimony. Next, the variability for each bioclim variable was plotted on separate MCC trees. However, we present only the reconstructions of BIO6, BIO10, and BIO15, as the climatic niche of Rhacophoridae is mostly defined by these three variables (PC1 axis). Moreover, to understand what the results obtained above for niche evolution means in terms of geography, we followed the code provided by Cobos et al.⁸⁵ and mapped niche evolution across BIO6 and BIO10, and BIO15 (Fig. 5).

We tested whether evolutionary rates of the main climatic niche axes (PC1, PC2, and PC3) differ significantly among species inhabiting different biogeographic regions, islands, mainland, and both islands and mainland. We assumed that species living both on islands and mainland have a broader climatic niche than only-island and only-mainland species; high rates of climatic niche evolution of those species would suggest NE. We used 1000 potential trait histories from stochastic character mapping and then fit two alternative models of evolution on each studied trait—one that fixes the rate of niche evolution to be identical between island/mainland inhabitants, and an alternative model in which the inhabitants have separate rates. We calculated the Akaike Information Criterion for small sample size (AICc) from the maximum likelihood estimate on each tree using the “brownie.lite” function in PHYTOOLS. Subsequently, we calculated model-averaged estimates of evolutionary rates for each category. Similarly, rates of climatic niche evolution associated with different reproductive modes were assessed using the above method.

Finally, to infer the biogeographic history of Rhacophoridae by determining whether lineages originated on islands or on the mainland, a model-testing approach was applied using the R package BioGeoBEARS v.0.2.1⁸⁶ based on the maximum credibility tree. Species occurrences were categorized according to the biogeographic areas modified from Chen et al.¹⁸: (1) Africa mainland; (2) peninsular India (mainland); (3) Sri Lanka (island); (4) East/Southeast Asia mainland; (5) East/Southeast Asian islands, including Japan, Taiwan, Hong kong and Hainan; (6) Sundaland (island archipelago); and (7) Himalaya. Given the extreme geological complexity of the region through time, dispersal constraints were not applied¹⁸. Analyses used six biogeographic models specified in the package: DEC—Dispersal-Extinction Cladogenesis; DIVALIKE—ML version of Dispersal Vicariance Analysis; BAYAREALIKE Bayesian biogeographical inference model; and an additional parameter (+J) for each of these models that simulate the process of founder-event speciation (Supplementary Table 9). Model fit was assessed using the Akaike Information Criterion (AIC) and Akaike weights⁸⁶.

Reporting summary. Further information on research design is available in the Nature Research Reporting Summary linked to this article.

Data availability

The authors declare that data supporting the findings of this study are available within the file Supplementary Data 1, and the additional data that support the findings of this study are publicly available online at www.amphibiaweb.org, <https://amphibiansoftheworld.amnh.org/index.php>, <https://datadryad.org/stash/dataset/doi:10.5061/dryad.2jm63xsk6>, <https://www.ncbi.nlm.nih.gov/genbank/>, <http://www.iucnredlist.org/technical-documents/spatial-data>, <https://www.gbif.org>, and <https://www.worldclim.org>. For Genbank accession numbers see Supplementary Table 7.

Code availability

All codes used in support of this publication are publicly available in specific R packages which we have mentioned in the reference list.

Received: 14 September 2021; Accepted: 17 March 2022;

Published online: 11 April 2022

References

- Purvis, A., Fritz, S. A., Rodríguez, J., Harvey, P. H. & Grenyer, R. The shape of mammalian phylogeny: patterns, processes and scales. *Philos. Trans. R. Soc. B* **366**, 2462–2477 (2011).
- Pyron, R. A. & Wiens, J. J. Large-scale phylogenetic analyses reveal the causes of high tropical amphibian diversity. *Proc. R. Soc. B* **280**, 20131622 (2013).
- Kennedy, J. D. et al. Does the colonization of new biogeographic regions influence the diversification and accumulation of clade richness among the Corvidae (Aves: Passeriformes)? *Evolution* **71**, 38–50 (2017).
- Barahona, R. S., Sauquet, H. & Magallón, S. The delayed and geographically heterogeneous diversification of flowering plant families. *Nat. Ecol. Evol.* **4**, 1232–1238 (2020).
- Stroud, J. T. & Losos, J. B. Ecological opportunity and adaptive radiation. *Annu. Rev. Ecol. Evol. Syst.* **47**, 507–532 (2016).
- Graham, C. H., Ron, S. R., Santos, J. C., Schneider, C. J. & Moritz, C. Integrating phylogenetics and environmental niche models to explore speciation mechanisms in dendrobatid frogs. *Evolution* **58**, 1781–1793 (2004).
- Duran, A., Meyer, A. L. S. & Pie, M. R. Climatic niche evolution in New World monkeys (Platyrrhini). *PLoS ONE* **8**, e83684 (2013).
- Pie, M. R. The macroevolution of climatic niches and its role in ant diversification: Evolution of ant climatic niches. *Ecol. Entomol.* **41**, 301–307 (2016).
- Pie, M. R., Campos, L. L. F., Meyer, A. L. S. & Duran, A. The evolution of climatic niches in squamate reptiles. *Proc. R. Soc. B* **284**, 20170268 (2017).
- Evans, M. E. K., Smith, S. A., Flynn, R. S. & Donoghue, M. J. Climate, niche evolution, and diversification of the “Bird-Cage” evening primroses (*Oenothera*, sections *Anogra* and *Kleinia*). *Am. Nat.* **173**, 225–240 (2009).
- Peterson, T. A. & Cohoon, K. P. Sensitivity of distributional prediction algorithms to geographic data completeness. *Ecol. Model.* **117**, 159–164 (1999).
- Wiens, J. J. & Graham, C. H. Niche conservatism: integrating evolution, ecology, and conservation biology. *Annu. Rev. Ecol. Evol. Syst.* **36**, 519–539 (2005).
- Wiens, J. J. et al. Niche conservatism as an emerging principle in ecology and conservation biology. *Ecol. Lett.* **13**, 1310–1324 (2010).
- Parmesan, C. & Yohe, G. A globally coherent fingerprint of climate change impacts across natural systems. *Nature* **421**, 37–42 (2003).
- AmphibiaWeb. *Information on Amphibian Biology and Conservation* (AmphibiaWeb, 2002).
- Frost, D. R. Amphibian species of the world. An online reference. Version 6.1 <https://amphibiansoftheworld.amnh.org/index.php> (2020).
- Li, J.-T. et al. Diversification of rhacophorid frogs provides evidence for accelerated faunal exchange between India and Eurasia during the Oligocene. *Proc. Natl Acad. Sci. USA* **110**, 3441–3446 (2013).
- Chen, J.-M. et al. An integrative phylogenomic approach illuminates the evolutionary history of Old World tree frogs (Anura: Rhacophoridae). *Mol. Phylog. Evol.* **145**, 106724 (2020).
- Meegaskumbura, M. et al. Patterns of reproductive-mode evolution in Old World tree frogs (Anura, Rhacophoridae). *Zool. Scr.* **44**, 509–522 (2015).
- Pan, T. et al. The reanalysis of biogeography of the Asian tree frog, *Rhacophorus* (Anura: Rhacophoridae): geographic shifts and climatic change influenced the dispersal process and diversification. *PeerJ* **5**, e3995 (2017).
- Condamine, F. L., Leslie, A. B. & Antonelli, A. Ancient islands acted as refugia and pumps for conifer diversity. *Cladistics* **33**, 69–92 (2017).
- Becerra, J. X. & Venable, D. L. Sources and sinks of diversification and conservation priorities for the Mexican tropical dry forest. *PLoS ONE* **3**, e3436 (2008).
- Grosjean, S., Delorme, M., Dubois, A. & Ohler, A. Evolution of reproduction in the Rhacophoridae (Amphibia, Anura). *J. Zool. Syst.* **46**, 169–176 (2008).
- Rolland, J. et al. The impact of endothermy on the climatic niche evolution and the distribution of vertebrate diversity. *Nat. Ecol. Evol.* **2**, 459–464 (2018).
- Zwickl, D. J. & Hillis, D. M. Increased taxon sampling greatly reduces phylogenetic error. *Syst. Biol.* **51**, 588–598 (2002).
- Chan, K. O. et al. Target-capture phylogenomics provide insights on gene and species tree discordances in Old World treefrogs (Anura: Rhacophoridae). *Proc. R. Soc. B* **287**, 20202102 (2020).
- Mishler, B. D. et al. Phylogenetic measures of biodiversity and neo- and paleoendemism in Australian Acacia. *Nat. Commun.* **5**, 4473 (2014).
- Myers, N. et al. Biodiversity hotspots for conservation priorities. *Nature* **403**, 853–858 (2000).
- Bain, R. et al. Amphibians of the Indomalayan realm. In *Threatened Amphibians of the World* (ed. Stuart, S. N.) Ch. 7 (Lynx Ediciones, 2008).
- De Bruyn, M. et al. Borneo and Indochina are major evolutionary hotspots for Southeast Asian biodiversity. *Syst. Biol.* **63**, 879–901 (2014).
- Meegaskumbura, M. et al. Sri Lanka: an amphibian hot spot. *Science* **298**, 379–379 (2002).
- Gorin, V. A. et al. A little frog leaps a long way: compounded colonizations of the Indian subcontinent discovered in the tiny Oriental frog genus *Microhyla* (Amphibia: Microhylidae). *PeerJ* **8**, e9411 (2020).
- Sillero, N. & Barbosa, A. M. Common mistakes in ecological niche models. *Internat. J. Geogr. Info Sci.* **35**, 1–14 (2020).
- Owens, H. L. & Guralnick, R. climateStability: an R package to estimate climate stability from time-slice climatologies. *Biodiv Inf.* **14**, 8–13 (2014).
- Fick, S. E. & Hijmans, R. J. WorldClim 2: new 1-km spatial resolution climate surfaces for global land areas. *Int. J. Climatol.* **37**, 4302–4315 (2017).
- Wiens, J. J., Kuczynski, C. A., Duellman, W. E. & Reeder, T. W. Loss and re-evolution of complex life cycles in marsupial frogs: does ancestral trait reconstruction mislead? *Evolution* **61**, 1886–1899 (2007).
- Chen, D. & Chen, H. W. Using the Köppen classification to quantify climate variation and change: an example for 1901–2010. *Environ. Devel.* **6**, 69–79 (2013).
- Pugliesi, L. & Rapini, A. Tropical refuges with exceptionally high phylogenetic diversity reveal contrasting phylogenetic structures. *Intern. J. Biodiv.* **2015**, 1–17 (2015).
- IUCN (International Union for Conservation of Nature). Rhacophoridae. The IUCN Red List of threatened species. Version 2020-3. <http://www.iucnredlist.org> (2019).
- Vilela, B. & Villalobos, F. letsR: a new R package for data handling and analysis in macroecology. *Meth. Ecol. Evol.* **6**, 1229–1234 (2015).
- Meegaskumbura, M. et al. Diversification of shrub frogs (Rhacophoridae, *Pseudophilautus*) in Sri Lanka—Timing and geographic context. *Mol. Phylog. Evol.* **132**, 14–24 (2019).
- Zachos, J. Trends, rhythms, and aberrations in global climate 65 Ma to present. *Science* **292**, 686–693 (2001).

43. Yao, Y.-F. et al. Reconstruction of paleovegetation and paleoclimate in the Early and Middle Eocene, Hainan Island, China. *Clim. Change* **92**, 169–189 (2009).
44. Kominz, M. A. et al. Late Cretaceous to Miocene sea-level estimates from the New Jersey and Delaware coastal plain coreholes: an error analysis. *Basin Resch* **20**, 211–226 (2008).
45. Vijayakumar, S. P., Menezes, R. C., Jayarajan, A. & Shanker, K. Glaciations, gradients, and geography: multiple drivers of diversification of bush frogs in the Western Ghats escarpment. *Proc. R. Soc. B* **283**, 20161011 (2016).
46. Licht, A. et al. Asian monsoons in a late Eocene greenhouse world. *Nature* **513**, 501–506 (2014).
47. Owen, L. A. & Dortch, J. M. Nature and timing of Quaternary glaciation in the Himalayan–Tibetan orogen. *Quat. Sci. Rev.* **88**, 14–54 (2014).
48. Spicer, R. A. et al. Why ‘the uplift of the Tibetan Plateau’ is a myth. *Natl Sci. Rev.* **8**, nwa091 (2021).
49. Klaus, S., Morley, R. J., Plath, M., Zhang, Y.-P. & Li, J.-T. Biotic interchange between the Indian subcontinent and mainland Asia through time. *Nat. Commun.* **7**, 12132 (2016).
50. Giorgioni, M. et al. Carbon cycle instability and orbital forcing during the Middle Eocene climatic optimum. *Sci. Rep.* **9**, 9357 (2019).
51. Owens, H. L. et al. Acknowledging uncertainty in evolutionary reconstructions of ecological niches. *Ecol. Evol.* **10**, 6967–6977 (2020).
52. Hall, R. Sundaland and Wallacea: geology, plate tectonics and palaeogeography. In *Biotic Evolution and Environmental Change in Southeast Asia* (eds Gower, D. J. et al.) Ch. 03 (Cambridge Univ. Press, 2012).
53. Snow, R. Continental climate and continentality. In *Encyclopedia of World Climatology* (ed. Oliver, J. E.) Ch. 58 (Springer, 2005).
54. Papadopoulou, A. & Knowles, L. L. Species-specific responses to island connectivity cycles: refined models for testing phylogeographic concordance across a Mediterranean Pleistocene aggregate island complex. *Mol. Ecol.* **24**, 4252–4268 (2015).
55. Weigelt, P., Jetz, W. & Kreft, H. Bioclimatic and physical characterization of the world’s islands. *Proc. Natl Acad. Sci. USA* **110**, 15307–15312 (2013).
56. Parrott, L. Measuring ecological complexity. *Ecol. Indic.* **10**, 1069–1076 (2010).
57. Sandel, B. et al. The influence of Late Quaternary climate-change velocity on species endemism. *Science* **334**, 660–664 (2011).
58. Strijk, J. S. et al. In and out of Madagascar: dispersal to peripheral islands, insular speciation and diversification of Indian Ocean daisy trees (*Psidium*, Asteraceae). *PLoS ONE* **7**, e42932 (2012).
59. Thomas, G. H. et al. PASTIS: an R package to facilitate phylogenetic assembly with soft taxonomic inferences. *Meth. Ecol. Evol.* **4**, 1011–1017 (2013).
60. Stamatakis, A. RAXML version 8: a tool for phylogenetic analysis and post-analysis of large phylogenies. *Bioinformatics* **30**, 1312–1313 (2014).
61. Zhang, C., Rabiee, M., Sayyari, E. & Mirarab, S. ASTRAL-III: polynomial time species tree reconstruction from partially resolved gene trees. *BMC Bioinf.* **19**, 153 (2018).
62. Edgar, R. C. MUSCLE: a multiple sequence alignment method with reduced time and space complexity. *BMC Bioinf.* **5**, 113 (2004).
63. Tamura, K., Stecher, G., Peterson, D., Filipski, A. & Kumar, S. MEGA6: molecular evolutionary genetics analysis version 6.0. *Mol. Biol. Evol.* **30**, 2725–2729 (2013).
64. Ronquist, F. et al. MrBayes 3.2: efficient Bayesian phylogenetic inference and model choice across a large model space. *Syst. Biol.* **61**, 539–542 (2012).
65. Paradis, E., Claude, J. & Strimmer, K. APE: analyses of phylogenetics and evolution in R language. *Bioinformatics* **20**, 289–290 (2004).
66. Orme, D. et al. caper: Comparative Analyses of Phylogenetics and Evolution in R version 0.5. <http://CRAN.R-project.org/package=caper> (2018).
67. Jetz, W., Thomas, G. H., Joy, J. B., Hartmann, K. & Mooers, A. O. The global diversity of birds in space and time. *Nature* **491**, 444–448 (2012).
68. Tonini, J. F. R., Beard, K. H., Ferreira, R. B., Jetz, W. & Pyron, R. A. Fully-sampled phylogenies of squamates reveal evolutionary patterns in threat status. *Biol. Cons.* **204**, 23–31 (2016).
69. Maestri, R. et al. The ecology of a continental evolutionary radiation: is the radiation of sigmodontine rodents adaptive?: evolutionary radiation on a continental scale. *Evolution* **71**, 610–632 (2017).
70. Nowakowski, A. J. et al. Phylogenetic homogenization of amphibian assemblages in human-altered habitats across the globe. *Proc. Natl Acad. Sci. USA* **115**, E3454–E3462 (2018).
71. Lanfear, R., Frandsen, P. B., Wright, A. M., Senfeld, T. & Calcott, B. PartitionFinder 2: new methods for selecting partitioned models of evolution for molecular and morphological phylogenetic analyses. *Mol. Biol. Evol.* **34**, 772–773 (2016).
72. Drummond, A. J., Suchard, M. A., Xie, D. & Rambaut, A. Bayesian phylogenetics with BEAUti and the BEAST 1.7. *Mol. Biol. Evol.* **29**, 1969–1973 (2012).
73. Rambaut, A. & Drummond, A. J. TreeAnnotator v1.10.4. Available as part of the BEAST package a <http://beast.bio.ed.ac.uk> (2013).
74. Harvey, M. G. & Rabosky, D. L. Continuous traits and speciation rates: alternatives to state-dependent diversification models. *Meth. Ecol. Evol.* **9**, 984–993 (2018).
75. Beaulieu, J. M. & O’Meara, B. C. Detecting hidden diversification shifts in models of trait-dependent speciation and extinction. *Syst. Biol.* **65**, 583–601 (2016).
76. Revell, L. J. phytools: an R package for phylogenetic comparative biology (and other things). *Meth. Ecol. Evol.* **3**, 217–223 (2012).
77. Faith, D. P. Conservation evaluation and phylogenetic diversity. *Biol. Cons.* **61**, 1–10 (1992).
78. Morlon, H. et al. RPANDA: an R package for macroevolutionary analyses on phylogenetic trees. *Meth. Ecol. Evol.* **7**, 589–597 (2016).
79. Chamberlain, S. et al. rgbif: interface to the global ‘Biodiversity’ information facility API. R package version 0.9.8. <https://CRAN.R-project.org/package=rgbif> (2020).
80. R Development Core Team. A language and environment for statistical computing: reference index. (R Foundation for Statistical Computing, 2010).
81. Hijmans, R. J. et al. raster: Geographic Data Analysis and Modeling (R package). <https://CRAN.R-project.org/package=raster> (2020).
82. Oksanen, J. et al. vegan: community ecology package. <https://github.com/vegandevs/vegan> (2019).
83. Harmon, L. J. Tempo and mode of evolutionary radiation in iguanian lizards. *Science* **301**, 961–964 (2003).
84. Harmon, L. J., Weir, J. T., Brock, C. D., Glor, R. E. & Challenger, W. GEIGER: investigating evolutionary radiations. *Bioinformatics* **24**, 129–131 (2008).
85. Cobos, M. E., Cheng, Y., Song, G., Lei, F. & Peterson, A. T. New distributional opportunities with niche innovation in Eurasian snowfinches. *J. Avian Biol.* **52**, jav.02868 (2021).
86. Matzke, N. J. BioGeoBEARS: BioGeography with Bayesian (and Likelihood) evolutionary analysis in R scripts. R package, version 0.2.1 (2013).

Acknowledgements

We thank Jayampathi Herath, Dan Sun, Ting Ru Mao, and Amrapali Rajput for their assistance in compiling earlier data. This work is published by a grant from the Museum of Comparative Zoology’s (Harvard University) Wetmore Colles Fund.

Author contributions

Conceptualization, investigation, data curation—G.E. and M.M.; Methodology—G.E., M.R.P., and M.M.; Formal analysis—G.E. and M.R.P.; Resources—R.P. and M.M.; Funding—J.H. and M.M.; Validation, Writing—original draft preparation, Writing—review and editing, G.E., M.R.P., J.H., R.P., and M.M.; Supervision—M.M.

Competing interests

The authors declare no competing interests.

Additional information

Supplementary information The online version contains supplementary material available at <https://doi.org/10.1038/s42003-022-03292-1>.

Correspondence and requests for materials should be addressed to Madhava Meegaskumbura.

Peer review information *Communications Biology* thanks Gregory Jongsma and the other, anonymous, reviewer(s) for their contribution to the peer review of this work. Primary Handling Editor: Luke R. Grinham.

Reprints and permission information is available at <http://www.nature.com/reprints>

Publisher’s note Springer Nature remains neutral with regard to jurisdictional claims in published maps and institutional affiliations.



Open Access This article is licensed under a Creative Commons Attribution 4.0 International License, which permits use, sharing, adaptation, distribution and reproduction in any medium or format, as long as you give appropriate credit to the original author(s) and the source, provide a link to the Creative Commons license, and indicate if changes were made. The images or other third party material in this article are included in the article’s Creative Commons license, unless indicated otherwise in a credit line to the material. If material is not included in the article’s Creative Commons license and your intended use is not permitted by statutory regulation or exceeds the permitted use, you will need to obtain permission directly from the copyright holder. To view a copy of this license, visit <http://creativecommons.org/licenses/by/4.0/>.

© The Author(s) 2022